ACS APPLIED MATERIALS & INTERFACES

Research Article

www.acsami.org

Mixed Self-Assembly of Polyethylene Glycol and Aptamer on Polydopamine Surface for Highly Sensitive and Low-Fouling Detection of Adenosine Triphosphate in Complex Media

Guixiang Wang,[†,‡] Qingjun Xu,[†] Lei Liu,[†] Xiaoli Su,[†] Jiehua Lin,[†] Guiyun Xu,[†] and Xiliang Luo*[,†]

[†]Key Laboratory of Sensor Analysis of Tumor Marker, Ministry of Education, College of Chemistry and Molecular Engineering, Qingdao University of Science and Technology, Qingdao 266042, China

[‡]College of Chemistry and Chemical Engineering, Taishan University, Taian 271021, China

Supporting Information

ABSTRACT: Detection of disease biomarkers within complex biological media is a substantial outstanding challenge because of severe biofouling and nonspecific adsorptions. Herein, a reliable strategy for sensitive and low-fouling detection of a biomarker, adenosine triphosphate (ATP) in biological samples was developed through the formation of a mixed self-assembled sensing interface, which was constructed by simultaneously self-assembling polyethylene glycol (PEG) and ATP aptamer onto the self-polymerized polydopamine-modified electrode surface. The developed aptasensor exhibited high selectivity and sensitivity toward the detection of ATP, and the linear range was 0.1−1000 pM, with a detection limit down to 0.1 pM. Moreover, owing to the presence of PEG within the sensing interface, the aptasensor was capable of sensing ATP in complex biological media such as human plasma with significantly reduced nonspecific adsorption effect. Assaying ATP in real biological samples including breast cancer cell lysates further proved the feasibility of this biosensor for practical application.

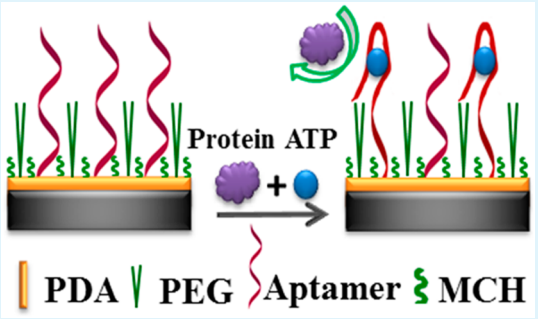

KEYWORDS: *antifouling, aptasensor, polyethylene glycol, polydopamine, cancer cell lysates, adenosine triphosphate*

1. INTRODUCTION

Early detection of disease biomarkers is extremely important in clinical diagnosis, and much attention has been paid to the development of new technologies to determine early signs of various diseases,[1,2] such as enzyme-linked immunosorbent assay,[3] fluorescense methods,[4,5] surface plasmon resonance,[6] surface enhanced Raman spectroscopy,[7] and so on. Among these, electrochemical technique has attracted much interest owing to its advantages such as high sensitivity, simple preparation, convenient operation, and low cost.[8−10] Currently, the sensitivity of electrochemical biosensors can be greatly improved by using signal amplification strategies,[11−14] but direct detection of targets in real complex media with electrochemical biosensors remains a challenge due to severe nonspecific adsorption.

Some efforts have been tried to resist nonspecific protein adsorption. For example, bovine serum albumin (BSA) was often used to block the biosensor surface in order to reduce the nonspecific adsorption or fouling effects.[15,16] Nevertheless, such BSA-protected surfaces only have limited antifouling properties to human blood serum or plasma, and blocking the surfaces may lead to a reduction in the recognition activity of immobilized bioreceptors.[17] In past years, certain materials with potential antifouling properties, such as polyethylene glycol (PEG) and zwitterionic materials, have been introduced into biosensors to improve their antifouling performances, and some positive results have been achieved.[18−20] In many cases, antifouling materials were used to modify the electrode as substrates first, and recognition probes were then immobilized on the surface of these materials.[21−24] During the biosensor construction process, normally the recognition probes were covalently attached to the antifouling materials, for instance, through the formation of amide bonds. This process will more or less alter the structure and charge of the antifouling materials, and thus weaken their ability to resist biofouling in some degree. Recently, Sun and co-workers have reported a sensitive and accurate method for detection of fructose in protein solutions, based on a mixed self-assembled monolayer consisting of *N*,*N*-dimethyl-cysteamine-carboxybetaine (a short zwitterioionic thiolated antifouling material) and 4-mercapto-phenylboronic acid (a fructose probe).[6] This strategy provided a simple and general model for antifouling biosensor fabrication, where the immobilization of recognition probes will not affect the antifouling material.

For the construction of electrochemical biosensors, preferred electrode substrates are those electrically conductive and readily for modification with biomolecules. Polydopamine (PDA) formed by the self-polymerization of dopamine (DA) under

Received: July 2, 2017
Accepted: August 23, 2017
Published: August 23, 2017

DOI: 10.1021/acsami.7b09529
ACS Appl. Mater. Interfaces 2017, 9, 31153−31160

alkaline condition (pH 8.5) has a strong adhesion to various inorganic and organic materials,[25−27] and it contains many functional groups such as quinone, catechol, amine, and imine, which are suitable for further modification. Moreover, PDA processes excellent biocompatibility and negligible cytotoxicity.[25] Therefore, PDA has attracted much attention in the construction of sensors and biosensors. The modification of electrodes with PDA and the further attachment of biomolecules to PDA have been widely explored. Martín and co-workers have reported the deposition of platinum onto a gold screen-printed electrode, and then followed by the electrodeposition of PDA directly on platinum to covalently immobilize cholesterol oxidase via Schiff base formation and Michael-type addition reaction.[9] Zhang and co-workers have fabricated an electrochemical DNA sensor based on the covalent immobilization of NH_2-terminated DNA probe onto PDA-modified electrode.[28] Core−shell Fe_3O_4@PDA magnetic nanoparticles have also been employed as solid supports for covalent immobilization of horseradish peroxidase to construct a highly sensitive biosensor for the detection of H_2O_2.[29]

Taking advantage of the unique property of PDA, we constructed herein a novel aptasensor based on the self-assembly of PEG and aptamer on PDA-modified electrode. Adenosine triphosphate (ATP), which plays a key role in the organisms and was regarded as an indicator for cell viability and injury,[30] was selected as the sensing target. The PDA self-polymerized on a glass carbon electrode (GCE) surface provided a good substrate for the assembly of antifouling polymer PEG and ATP aptamer via the Michael addition reaction, as illustrated in Scheme S1.[25] Owing to the presence of PEG in the sensing interface, the prepared aptasensor was capable of detecting ATP in human plasma and cancer cell lysates.

2. EXPERIMENTAL SECTION

2.1. Reagents. ATP, adenosine monophosphate (AMP), adenosine diphosphate (ADP), guanosine triphosphate (GTP), uridine triphosphate (UTP), and cytosine triphosphate (CTP) were all purchased from the Thermo Scientific, USA. The ATP binding aptamer [5′-SH-$(CH_2)_6$-ACC TGG GGG AGT ATT GCG GAG GAA GGT] was purchased from the Sangon Biotech Co., Ltd. (Shanghai, China), which was purified by high-performance liquid chromatography and used as received. DA, lysozyme (Lys), β-lactoglobulin (β-LG), BSA, and 6-mercaptohexanol (MCH) were purchased from Taitan Sci. Co. Ltd. (Shanghai, China). PEG terminated with thiol group (M_n 2000) was obtained from Xiamen Sinopeg Biotech. Co., Ltd. (Xiamen, China). Human plasma samples were provided by the Hospital of Taishan University, China. Other reagents were of analytical grade. Millipore water with a resistivity greater than 18 MΩ cm was used in all experiments.

2.2. Apparatus. Electrochemical experiments were carried out with an electrochemical workstation (CHI650E, Shanghai Chenhua Instrument Co. Ltd., China). A conventional three-electrode system was employed in all electrochemical measurements with a GCE (diameter 3.0 mm), a saturated calomel electrode (SCE), and a platinum wire electrode. All measurements were performed at room temperature. Atomic force microscopy (AFM) images were recorded on an Agilent 550 AFM (Agilent Technologies) in tapping mode. X-ray photoelectron spectroscopy (XPS) measurements were carried out with a Thermo-VG Scientific ESCALAB 250Xi spectrometer with a monochromatic Al Kα X-ray source. The contact angle was measured with a contact angle goniometer (JC2000, Zhongchen Digital Technical Co., Shanghai, China) by the sessile drop method.

2.3. Fabrication of the Electrochemical Aptasensor. The aptasensor was prepared as shown in Scheme 1. GCE was polished using alumina slurries with the diameter of 1.0, 0.3, and 0.05 μm, respectively, followed by ultrasonic cleaning with water, absolute ethanol and water for 3 min in sequence. The cleaned GCE was immersed in the DA solution (2 mg/mL) containing Tris buffer (10 mM, pH 8.5) for 50 min, and it was then adequately rinsed with water and Tris buffer (50 mM, pH 8.5) in sequence. Subsequently, 10 μL of solution (50 mM Tris buffer, pH 8.5) containing 1 μM aptamer and 5 mg/mL PEG was dropped on the electrode surface for overnight incubation at ambient temperature. The Tris buffer was fully degassed with nitrogen before use to prevent the oxidation of thiol groups of aptamer and PEG into disulfide bonds,[31] and the electrode was covered and sealed with a wet beaker (filled with nitrogen gas) to prevent the solution from evaporating. In order to block the uncovered surface of the electrode, it was immersed in phosphate-buffered saline (PBS, 10 mM, pH 7.4) containing 1.0 mM MCH for 1 h at room temperature, followed by rinsing with Milliprore water.

Scheme 1. Schematic Illustration of the Fabrication of Aptasensor and Its Application to Label-Free Detection of ATP

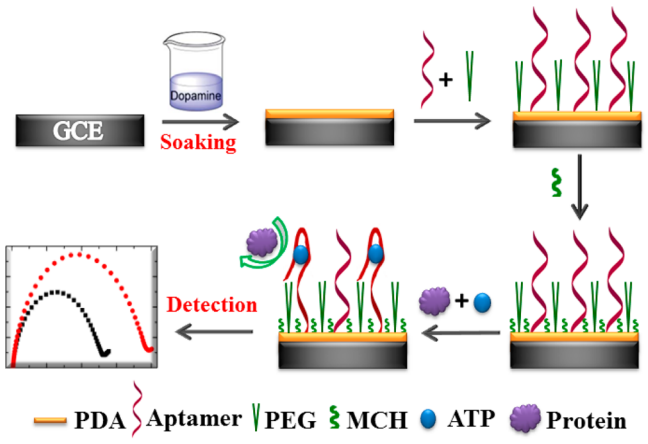

2.4. Electrochemical Impedance Spectroscopy (EIS) Measurements. EIS is an effective technique to monitor the changes happened at sensor surfaces, and it can transfer the complicated biorecognition process into sensitive electrical signals.[2] EIS measurements were recorded in PBS (10 mM, pH 7.4) containing 5.0 mM $[Fe(CN)_6]^{3-/4-}$ solution and 0.1 M KCl. The direct current potential was set at 0.20 V. The frequency range was from 0.1 to 10^5 Hz, and the amplitude of the applied sine wave was 5 mV. In this work, the Nyquist plot of EIS is used, which is composed of a semicircle portion at higher frequencies and a linear portion at low frequencies. The former corresponds to typical fingerprints of charge transfer (its semicircle diameter is equivalent to the charge transfer resistance (R_{ct})), while the latter relates to the diffusion limited process at the electrode interface.[32]

2.5. Extraction of ATP from Cancer Cells. ATP extraction from 4T1 breast cancer cells was performed according to a previous literature.[30] First, 8.71 × 10^5 cells (3 mL) determined by a hemocytometer were dispersed in Roswell Park Memorial Institute cell media buffer, centrifuged (5 min, 1000 rpm), washed with PBS for five times, and resuspended in Millipore water (0.25 mL). Then, the collected cells were disrupted by ultrasonic cell disruptor for 20 min (keeping the temperature at 0 °C). Finally, the lysates were centrifuged (at 18 000 rpm for 20 min at 4 °C) to get rid of cell debris.

3. RESULTS AND DISCUSSION

3.1. Characterization of the Modified Electrodes. XPS was used to characterize the surface composition of glassy carbon after different modification steps. Figure 1 illustrates the XPS survey scans of bare, PDA-coated, and Aptamer-PEG/PDA coated glassy carbon substrate. Carbon (C), nitrogen (N), and oxygen (O) are the nonmetal elements of the glassy carbon, and their photoelectron peaks appear at 285 eV (C_{1S}),

DOI: 10.1021/acsami.7b09529
ACS Appl. Mater. Interfaces 2017, 9, 31153−31160

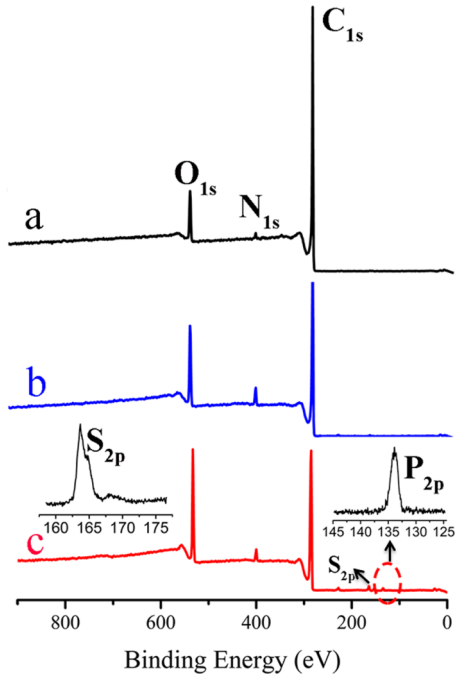

Figure 1. XPS spectra of (a) bare, (b) PDA film, and (c) Aptamer-PEG/PDA-modified glassy carbon.

400 eV (N_{1S}), and 533 eV (O_{1S}), respectively[31] (Figure 1a). After soaking in the DA solution, the peak intensities of N_{1s} and O_{1s} become stronger than those of the bare glassy carbon, while the peak intensity of C_{1s} becomes weaker than that of the bare glassy carbon, indicating that the surface was successfully coated with a PDA film (Figure 1b). After aptamer and PEG immobilization, two characteristic peaks appear. One peak appears at 134 eV, representing phosphorus 2p signal (P_{2p}) from aptamer (Figure 1c, right inset),[33] and the other peak appears at 164 eV, corresponding to the sulfur 2p (S_{2p}) signal coming from the surface-immobilized thiolated aptamer and PEG together (Figure 1c, left inset).[34]

To further characterize the PDA- and aptamer-PEG-modified surfaces, AFM was used to monitor the heights of different surfaces. As shown in Figure 2, the PDA film shows a relatively uniform and flat surface with an average height of about 2 nm, which is higher than that of the bare silicon wafer (about 0.1 nm) while much lower than that of the aptamer-PEG/PDA film (about 18.8 nm). This result indicates that PDA can be formed on the wafer surface, and further attachment of PEG and aptamer terminated with thiol group to the PDA can also be realized.

The surface wettability of electrode surfaces modified with different materials was characterized by static water contact angle method. As shown in Figure 3, the contact angle value of silicon wafer is about 30°. After PDA modification, the value increases to about 49°, which is in accordance with previously reported value.[31] Interestingly, the electrode surface immobilized with PEG and aptamer becomes very hydrophilic, and the contact angle is just about 20°, which may be ascribed to the presence of PEG with excellent hydrophilicity on the modified surface.

3.2. Electrochemical Characterization of the Aptasensor Fabrication Process. The fabrication process of the aptasensor was monitored using EIS and cyclic voltammograms (CVs), as shown in Figure 4. Compared with the bare GCE (Figure 4A, curve a), the PDA-modified electrode showed much higher R_{ct} (Figure 4A, curve b), which may be ascribed to the fact that PDA retards the interfacial electron transfer as its conductivity is poor. When the aptamer and PEG were attached to the PDA film simultaneously, R_{ct} increased remarkably (Figure 4A, curve c) owing to two factors: (1) The negatively charged phosphate skeletons of the aptamer will repel the negatively charged $[Fe(CN)_6]^{3-/4-}$ probe from approaching the electrode surface. (2) PEG can block the interfacial electron transfer owing to its poor conductivity. With MCH assembled on the PDA film, R_{ct} increased accordingly (Figure 4A, curve d), indicating successful blocking of the residual active sites of the PDA film with MCH. Interestingly, after incubation with ATP (ATP binding to the aptamer), R_{ct} of the modified electrode increased significantly (Figure 4A, curve e), which may be used as the signal for ATP sensing. The reason for this

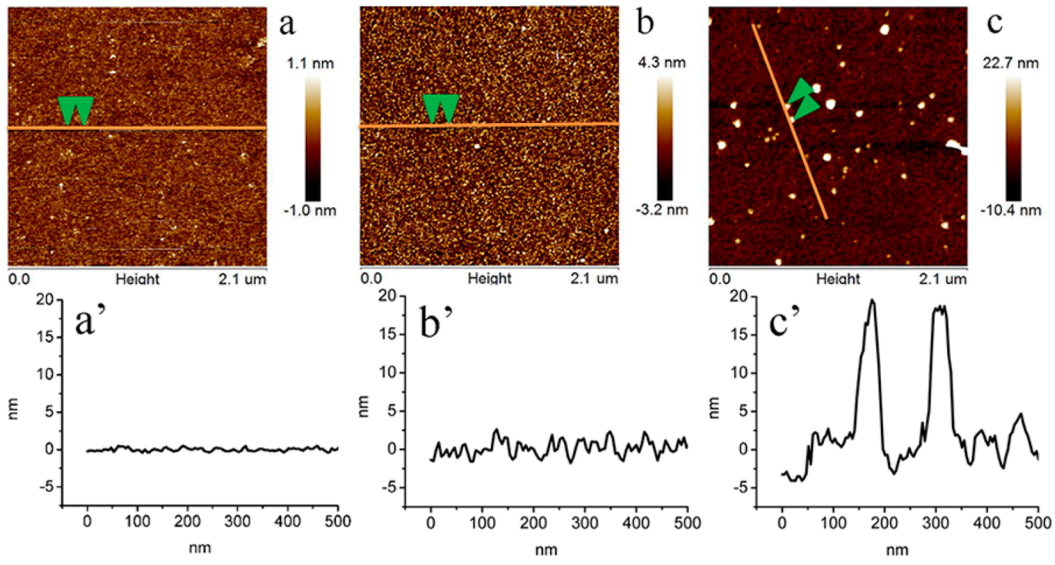

Figure 2. AFM images of silicon wafer (a), PDA film (b), and Aptamer-PEG/PDA (c) modified silicon wafers. The corresponding height profiles are shown in a′–c′, respectively.

DOI: 10.1021/acsami.7b09529
ACS Appl. Mater. Interfaces 2017, 9, 31153–31160

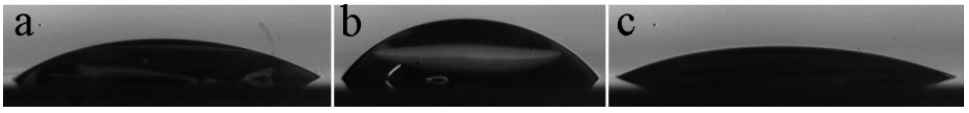

Figure 3. Images of water droplets on silicon wafer (a), PDA (b), and Aptamer-PEG/PDA (c) modified surfaces. The contact angle was (a) (30 ± 1)°, (b) (49 ± 2)°, and (c) (20 ± 2)°, respectively (n = 3).

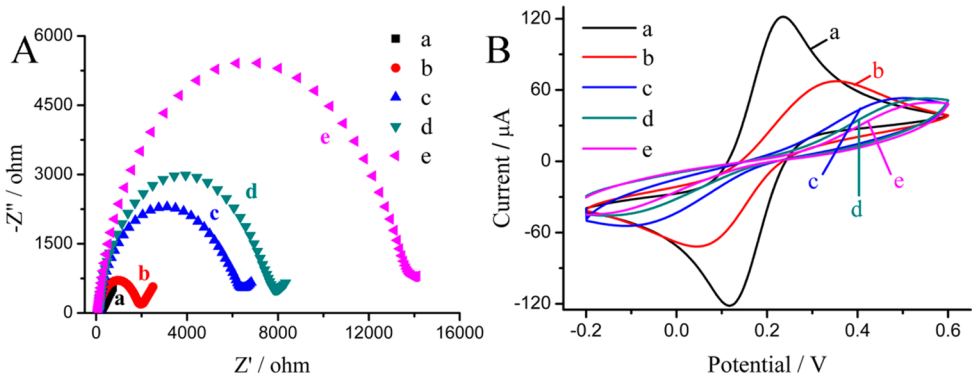

Figure 4. Impedance Nyquist plots of the EIS (A) and CV curves (B) obtained at different modified electrodes: (a) GCE; (b) PDA/GCE; (c) Aptamer-PEG/PDA/GCE; (d) MCH/Aptamer-PEG/PDA/GCE; and (e) ATP/MCH/Aptamer-PEG/PDA/GCE. Measurements were performed in PBS (10 mM, pH 7.4) containing 5.0 mM $[Fe(CN)_6]^{3-/4-}$ and 0.1 M KCl. The concentration of ATP was 0.1 μM (10 mM PBS, pH 7.4).

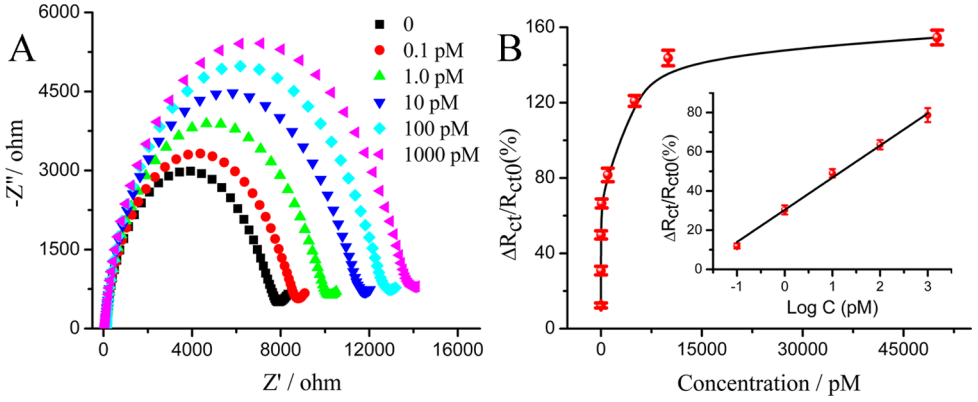

Figure 5. (A) Typical EIS response corresponding to the aptasensor incubated with different ATP concentrations (PBS, 10 mM, pH 7.4): curves from inner to outer represent 0, 0.1, 1, 10, 100, and 1000 pM ATP, respectively. (B). Charge-transfer resistance changes $[\Delta R_{ct}/R_{ct0}$ (%)] of the aptasensor based ATP biosensor upon a function of ATP concentrations. Inset: the corresponding standard curve of the aptasensor after the deduction of the background signal value. Error bars represent the standard deviations of three repeated determinations.

increase in R_{ct} may be ascribed to the fact that ATP carries negative phosphate groups, and its binding to the electrode surface will enhance the repulsion to the negative $[Fe(CN)_6]^{3-/4-}$ probe. The results of CV data (Figure 4B) were in accordance with the EIS characterization, further confirming the successful fabrication of the aptasensor.

3.3. Optimization of the ATP Incubation Time. Incubation time is an important parameter for the specific binding between aptamer and ATP. To maximize the sensitivity of the aptasensor, the incubation time was optimized using EIS, as shown in Figure S1. It can be clearly observed that the R_{ct} change $[\Delta R_{ct}/R_{ct0}$ (%)] increased with the increasing of the incubation time and reached a maximum at 1.5 h, indicating that the binding between the aptamer and ATP achieved equilibrium. Therefore, the optimal incubation time for this aptasensor was selected as 1.5 h.

3.4. Analytical Performance of the Aptasensor. The electrochemical sensing performance of the aptasensor for the label-free determination of ATP was investigated in PBS (10 mM, pH 7.4) by EIS. To ensure that the highly sensitive response of the aptasensor was originated from the binding of ATP, signal changes of the aptasensor incubated in PBS without ATP have been investigated, serving as a control. As shown in Figure S2, the $[\Delta R_{ct}/R_{ct0}$ (%)] value of the aptasensor without ATP had little change over time. Along with the increase of the ATP, R_{ct} increased accordingly (Figure 5A), and $[\Delta R_{ct}/R_{ct0}$ (%)] has a good linear relationship between the aptasensor response and the logarithm of the ATP concentration from 0.1 to 1000 pM (Figure 5B, the background signal value has been deducted). The regression equation is $\Delta R_{ct}/R_{ct0}$ (%) = 16.40 log C (pM) + 30.36 (R = 0.9978), and the limit of detection is approximately 0.1 pM (based on a signal-to-noise ratio of 3), which is much lower than that achieved in previous reports[35−40] and is close to that of Tang's work[41] (summarized in Table S1). Such a low detection limit may be mainly attributed to the unique structure of the sensing interface, where the PDA and PEG can provide a good environment for the ATP aptamer to retain high bioactivity and binding affinity.

3.5. Specificity and Reproducibility of the Aptasensor. To evaluate the binding specificity of the aptasensor to its

DOI: 10.1021/acsami.7b09529
ACS Appl. Mater. Interfaces 2017, 9, 31153−31160

target ATP, R_{ct} change of the aptasensor was measured in various solutions containing GTP, UTP, CTP, AMP, ADP, and ATP. As illustrated in Figure 6, compared with R_{ct} change to ATP, the fabricated aptasensor showed negligible signal response to GTP, UTP, CTP, AMP, and ADP. The results are in agreement with those reported in the literature,[35,39] indicating that the aptasensor has excellent selectivity for ATP determination. When AMP and ADP are at much higher concentrations, they may generate certain interference on the detection of ATP, and certain techniques such as dual recognition unit strategy[42] may be used to improve the biosensor selectivity.

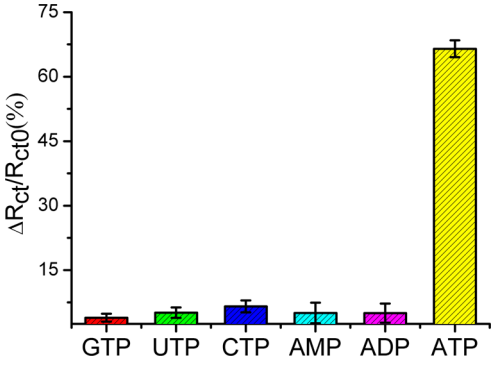

Figure 6. Responses of the aptasensor to GTP (1.0 nM), UTP (1.0 nM), CTP (1.0 nM), AMP (0.1 nM), ADP (0.1 nM), and ATP (0.1 nM). The error bars represent the standard deviation of three measurements.

To assess the reproducibility of the aptasensor, the relative standard deviations (RSDs) of the inter- and intra-assay were tested. Seven different electrodes prepared under the same experimental conditions were employed for the detection of 1.0 nM ATP, and the RSD was 6.75%. The same aptasensor was employed to detect 1.0 nM ATP for seven reduplicate measurements, and the RSD was 3.12%. These results indicated that the reproducibility of the aptasensor was acceptable.

3.6. Antifouling Property of the Aptasensor. As the aptasensor was developed based on the PDA substrate, the antifouling property of PDA was tested, as shown in Figure S3. Besides the main function to immobilize biomolecules terminated with thiol groups, PDA also showed certain antifouling ability to single proteins (BSA and Lys at low

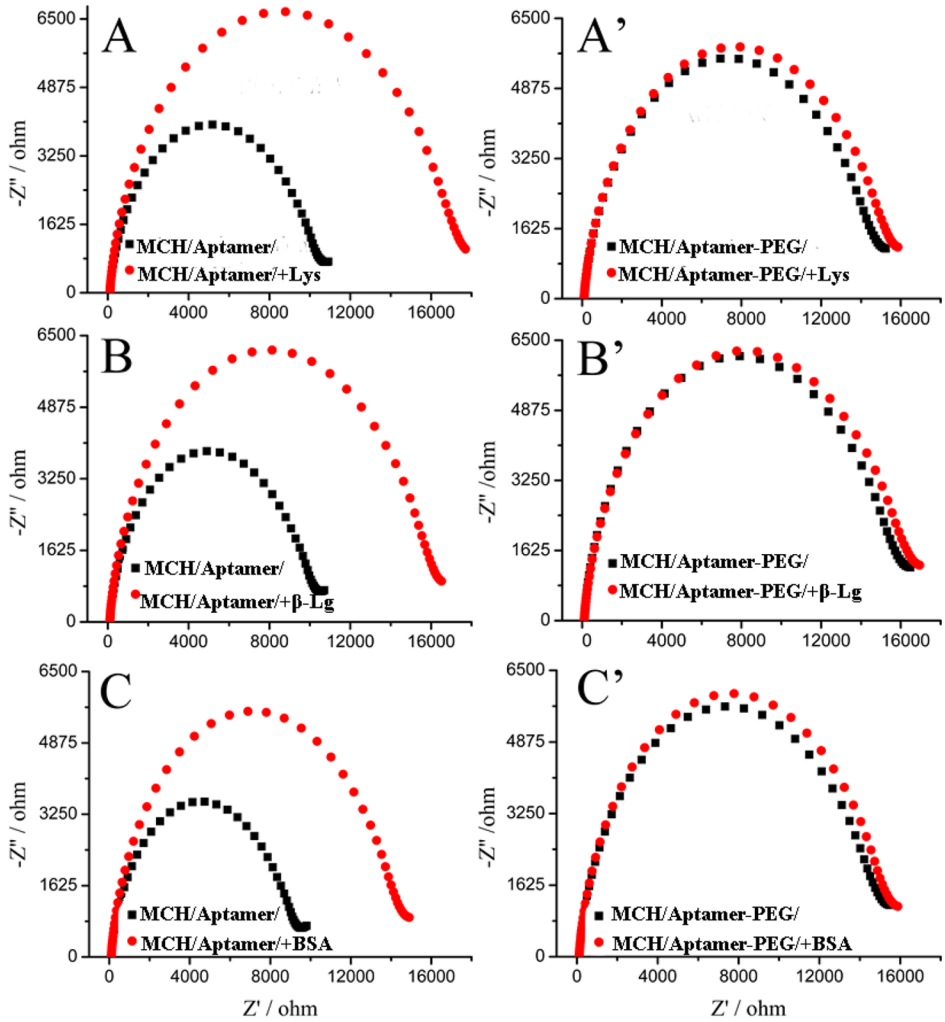

Figure 7. EIS of the aptasensor MCH/Aptamer/PDA/GCE without PEG (A–C) and MCH/Aptamer-PEG/PDA/GCE with PEG (A′–C′) before (■) and after (●) incubation with different proteins. (A and A′) incubation with Lysozyme (Lys); (B and B′) incubation with β-lactoglobulin (β-Lg); and (C and C′) incubation with bovine serum albumin (BSA). The protein concentration was 0.5 mg·mL^{-1}.

DOI: 10.1021/acsami.7b09529
ACS Appl. Mater. Interfaces 2017, 9, 31153–31160

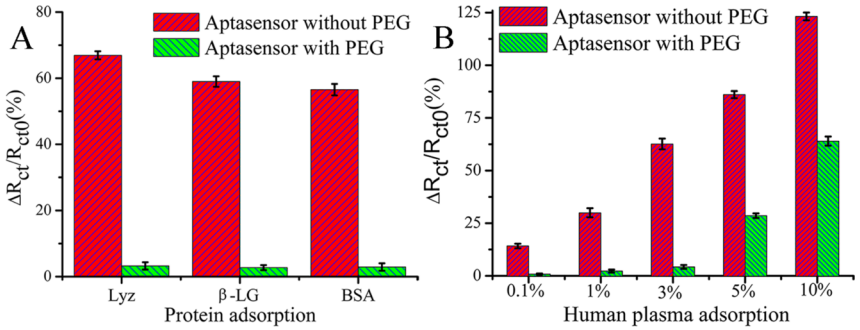

Figure 8. Charge-transfer resistance changes [$\Delta R_{ct}/R_{ct0}$ (%)] of the aptasensor with or without PEG after incubated in different proteins (A) and human plasma (B). Human plasma was diluted (V/V) with 10 mM pH 7.4 PBS containing 150 mM NaCl. The aptasensor with and without PEG corresponds to MCH/Aptamer-PEG/PDA/GCE and MCH/Aptamer/PDA/GCE, respectively.

concentrations) and highly diluted plasma, but its antifouling performance was very limited.

To assess the antifouling ability of the aptasensor, its resistance changes after incubating in single protein solutions (Lys, β-Lg, and BSA) (EIS changes as shown in Figure 7) and human plasma were recorded, respectively. To avoid possible response change related to ATP binding, the aptasensor was saturated with ATP before incubating in human plasma. As can be seen in Figures 7 and 8, the aptasensor with PEG showed significantly smaller resistance change owing to nonspecific adsorption compared with that of the sensor without PEG, whether soaking in single protein solutions or in human plasma, which suggested promising antifouling ability of the biosensor with PEG.[20,43]

3.7. Clinical Application of the Aptasensor. *3.7.1. Detection of ATP in Human Blood Plasma.* To investigate the practical application of the developed ATP aptasensor, the performance of the aptasensor in 3% human plasma samples were tested by standard addition method. Various concentrations of ATP were added into 3% human plasma samples before measuring. The experimental results were summarized in Table S2 (see the Supporting Information), and the recovery was ranging from 98.40 to 106.10%, with RSD between 2.71 and 4.18%, showing great potential for specific determination of ATP in biological fluids.

3.7.2. Detection of ATP in Cancer Cell Extracts. To further demonstrate that the aptasensor was applicable to real samples, this biosensor was applied to detect ATP in 4T1 breast cancer cell lysates. Before measuring, the cell lysates were filtrated using cutoff membranes (cut off 10 KD) to remove small cell debris and then diluted with PBS for EIS measurements. The aptasensor was incubated in the diluted cell lysates for 1.5 h at 37 °C. The concentration of ATP in the breast cancer cell lysate was detected and calculated to be 0.29 (±0.02) mM (n = 3) with the aptasensor, which is very close to the value of 0.27 (±0.02) mM measured by HPLC method (Table S3).

4. CONCLUSION

A novel aptasensor for ultrasensitive, label-free, and low-fouling detection of ATP in biological fluids was developed based on self-polymerized PDA substrate anchored with PEG and aptamer. PEG and aptamer terminated with thiol group can be effectively immobilized to PDA film via Michael addition reaction under mild conditions. In the constructed sensing interface, PEG can provide a biocompatible environment for aptamer to remain high binding affinity, and at the same time, it exhibits resistance to nonspecific protein adsorption, making the aptasensor highly sensitive and low-fouling. The aptasensor can be used to assay ATP in human plasma and cell lysates with satisfying accuracy and without suffering from biofouling, suggesting great potential for practical application.

■ ASSOCIATED CONTENT

Supporting Information

The Supporting Information is available free of charge on the ACS Publications website at DOI: 10.1021/acsami.7b09529.

Michael addition reaction mechanism, optimization of ATP incubation, control experiment for detecting ATP, comparison of sensing performances for ATP detection, antifouling performance of PDA, analytical results for ATP in real samples and the results compared with HPLC method (PDF)

■ AUTHOR INFORMATION

Corresponding Author

*E-mail: xiliangluo@qust.edu.cn. Fax: +8653284022681. Tel.: +86 53284022860.

ORCID

Xiliang Luo: 0000-0001-6075-7089

Notes

The authors declare no competing financial interest.

■ ACKNOWLEDGMENTS

This research was supported by the Natural Science Foundation of Shandong Province of China (JQ201406), the National Natural Science Foundation of China (21422504, 21675093), and the Taishan Scholar Program of Shandong Province of China (ts20110829).

■ REFERENCES

(1) Wang, Y. G.; Zhang, Y.; Wu, D.; Ma, H. M.; Pang, X. H.; Fan, D. W.; Wei, Q.; Du, B. Ultrasensitive Label-free Electrochemical Immunosensor Based on Multifunctionalized Graphene Nanocomposites for the Detection of Alpha Fetoprotein. *Sci. Rep.* **2017**, *7*, 42361.

(2) Wu, L.; Qu, X. G. Cancer Biomarker Detection: Recent Achievements and Challenges. *Chem. Soc. Rev.* **2015**, *44*, 2963−2997.

(3) Alberti, D.; van't Erve, M.; Stefania, R.; Ruggiero, M. R.; Tapparo, M.; Geninatti Crich, S.; Aime, S. A Quantitative Relaxometric Version of the ELISA Test for the Measurement of Cell Surface Biomarkers. *Angew. Chem., Int. Ed.* **2014**, *53*, 3488−3491.

(4) Chinen, A. B.; Guan, C. M.; Ferrer, J. R.; Barnaby, S. N.; Merkel, T. J.; Mirkin, C. A. Nanoparticle Probes for the Detection of Cancer Biomarkers, Cells, and Tissues by Fluorescence. *Chem. Rev.* **2015**, *115*, 10530−10574.

DOI: 10.1021/acsami.7b09529
ACS Appl. Mater. Interfaces 2017, 9, 31153−31160

(5) Xu, S.; Dong, B.; Zhou, D.; Yin, Z.; Cui, S.; Xu, W.; Chen, B.; Song, H. Paper-based Upconversion Fluorescence Resonance Energy Transfer Biosensor for Sensitive Detection of Multiple Cancer Biomarkers. *Sci. Rep.* **2016**, *6*, 23406.
(6) He, L.; Pagneux, Q.; Larroulet, I.; Serrano, A. Y.; Pesquera, A.; Zurutuza, A.; Mandler, D.; Boukherroub, R.; Szunerits, S. Label-free Femtomolar Cancer Biomarker Detection in Human Serum Using Graphene-coated Surface Plasmon Resonance Chips. *Biosens. Bioelectron.* **2017**, *89*, 606−611.
(7) Sun, F.; Ella-Menye, J.-R.; Galvan, D. D.; Bai, T.; Hung, H.-C.; Chou, Y.-N.; Zhang, P.; Jiang, S.; Yu, Q. Stealth Surface Modification of Surface-enhanced Raman Scattering Substrates for Sensitive and Accurate Detection in Protein Solutions. *ACS Nano* **2015**, *9*, 2668−2676.
(8) Wang, X.; Lin, G.; Cui, G.; Zhou, X.; Liu, G. L. White Blood Cell Counting on Smartphone Paper Electrochemical Sensor. *Biosens. Bioelectron.* **2017**, *90*, 549−557.
(9) Martín, M.; Salazar, P.; Álvarez, R.; Palmero, A.; López-Santos, C.; González-Mora, J. L.; González-Elipe, A. R. Cholesterol Biosensing with a Polydopamine-modified Nanostructured Platinum Electrode Prepared by Oblique angle Physical Vacuum Deposition. *Sens. Actuators, B* **2017**, *240*, 37−45.
(10) Labib, M.; Sargent, E. H.; Kelley, S. O. Electrochemical Methods for the Analysis of Clinically Relevant Biomolecules. *Chem. Rev.* **2016**, *116*, 9001−9090.
(11) Huo, X. H.; Liu, X. Q.; Liu, J.; Sukumaran, P.; Alwarappan, S.; Wong, D. K. Y. Strategic Applications of Nanomaterials as Sensing Platforms and Signal Amplification Markers at Electrochemical Immunosensors. *Electroanalysis* **2016**, *28*, 1730−1749.
(12) Zhao, L.; Ma, Z. New Immunoprobes **B**ased on Bovine Serum Albumin-stabilized Copper Nanoclusters with Triple Signal Amplification for Ultrasensitive Electrochemical Immunosensing for Tumor Marker. *Sens. Actuators, B* **2017**, *241*, 849−854.
(13) He, Y.; Xie, S.; Yang, X.; Yuan, R.; Chai, Y. Electrochemical Peptide Biosensor Based on in Situ Silver Deposition for Detection of Prostate Specific Antigen. *ACS Appl. Mater. Interfaces* **2015**, *7*, 13360−13366.
(14) Zhu, Q.; Chai, Y.; Zhuo, Y.; Yuan, R. Ultrasensitive Simultaneous Detection of Four Biomarkers Based on Hybridization Chain Reaction and Biotin−streptavidin Signal Amplification Strategy. *Biosens. Bioelectron.* **2015**, *68*, 42−48.
(15) Yang, Z.-H.; Zhuo, Y.; Yuan, R.; Chai, Y.-Q. An Amplified Electrochemical Immunosensor Based on in Situ-Produced 1-Naphthol as Electroactive Substance and Graphene Oxide and Pt Nanoparticles Functionalized CeO_2 Nanocomposites as Signal Enhancer. *Biosens. Bioelectron.* **2015**, *69*, 321−327.
(16) Jiang, X.; Wang, H.; Yuan, R.; Chai, Y. Sensitive Electrochemiluminescence Detection for CA15−3 Based on Immobilizing Luminol on Dendrimer Functionalized ZnO Nanorods. *Biosens. Bioelectron.* **2015**, *63*, 33−38.
(17) Lowe, S.; O'Brien-Simpson, N. M.; Connal, L. A. Antibiofouling Polymer Interfaces: Poly(ethylene glycol) and Other Promising Candidates. *Polym. Chem.* **2015**, *6*, 198−212.
(18) Liu, B.; Liu, X.; Shi, S.; Huang, R.; Su, R.; Qi, W.; He, Z. Design and Mechanisms of Antifouling Materials for Surface Plasmon Resonance Sensors. *Acta Biomater.* **2016**, *40*, 100−118.
(19) Vaisocherová, H.; Brynda, E.; Homola, J. Functionalizable Low-fouling Coatings for Label-free Biosensing in Complex Biological Media: Advances and Applications. *Anal. Bioanal. Chem.* **2015**, *407*, 3927−3953.
(20) Leng, C.; Hung, H.-C.; Sun, S.; Wang, D.; Li, Y.; Jiang, S.; Chen, Z. Probing the Surface Hydration of Nonfouling Zwitterionic and PEG Materials in Contact with Proteins. *ACS Appl. Mater. Interfaces* **2015**, *7*, 16881−16888.
(21) Hui, N.; Sun, X.; Niu, S.; Luo, X. PEGylated Polyaniline Nanofibers: Antifouling and Conducting Biomaterial for Electrochemical DNA Sensing. *ACS Appl. Mater. Interfaces* **2017**, *9*, 2914−2923.
(22) Luo, X.; Xu, Q.; James, T.; Davis, J. J. Redox and Label-free Array Detection of Protein Markers in Human Serum. *Anal. Chem.* **2014**, *86*, 5553−5558.
(23) Luo, X.; Xu, M.; Freeman, C.; James, T.; Davis, J. J. Ultrasensitive Label Free Electrical Detection of Insulin in Neat Blood Serum. *Anal. Chem.* **2013**, *85*, 4129−4134.
(24) Brault, N. D.; White, A. D.; Taylor, A. D.; Yu, Q.; Jiang, S. Directly Functionalizable Surface Platform for Protein Arrays in Undiluted Human Blood Plasma. *Anal. Chem.* **2013**, *85*, 1447−1453.
(25) Liu, Y.; Ai, K.; Lu, L. Polydopamine and Its Derivative Materials: Synthesis and Promising Applications in Energy, Environmental, and Biomedical Fields. *Chem. Rev.* **2014**, *114*, 5057−5115.
(26) Kim, S.; Gim, T.; Kang, S. M. Versatile, Tannic Acid-Mediated Surface PEGylation for Marine Antifouling Applications. *ACS Appl. Mater. Interfaces* **2015**, *7*, 6412−6416.
(27) Martín, M.; Salazar, P.; Jiménez, C.; Lecuona, M.; Ramos, M. J.; Ode, J.; Alcoba, J.; Roche, R.; Villalonga, R.; Campuzano, S.; Pingarrón, J. M.; González-Mora, J. L. Rapid Legionella Pneumophila Determination Based on a Disposable Core−shell Fe_3O_4@poly-(dopamine) Magnetic Nanoparticles Immunoplatform. *Anal. Chim. Acta* **2015**, *887*, 51−58.
(28) Zhang, Y.; Geng, X.; Ai, J.; Gao, Q.; Qi, H.; Zhang, C. Signal Amplification Detection of DNA Using a Sensor Fabricated by One-Step Covalent Immobilization of Amino-Terminated Probe DNA onto the Polydopamine-Modified Screen-printed Carbon Electrode. *Sens. Actuators, B* **2015**, *221*, 1535−1541.
(29) Martin, M.; Salazar, P.; Villalonga, R.; Campuzano, S.; Pingarron, J. M.; Gonzalez-Mora, J. L. Preparation of Core-shell Fe_3O_4@poly(dopamine) Magnetic Nanoparticles for Biosensor Construction. *J. Mater. Chem. B* **2014**, *2*, 739−746.
(30) Zhang, S.; Yan, Y.; Bi, S. Design of Molecular Beacons as Signaling Probes for Adenosine Triphosphate Detection in Cancer Cells Based on Chemiluminescence Resonance Energy Transfer. *Anal. Chem.* **2009**, *81*, 8695−8701.
(31) Cui, J.; Ju, Y.; Liang, K.; Ejima, H.; Lorcher, S.; Gause, K. T.; Richardson, J. J.; Caruso, F. Nanoscale Engineering of Low-fouling Surfaces Through Polydopamine Immobilisation of Zwitterionic Peptides. *Soft Matter* **2014**, *10*, 2656−2663.
(32) Cui, M.; Song, Z.; Wu, Y.; Guo, B.; Fan, X.; Luo, X. A Highly Sensitive Biosensor for Tumor Maker Alpha Fetoprotein Based on Poly (ethylene glycol) Doped Conducting Polymer PEDOT. *Biosens. Bioelectron.* **2016**, *79*, 736−741.
(33) Wang, G.; Han, R.; Su, X.; Li, Y.; Xu, G.; Luo, X. Zwitterionic Peptide Anchored to Conducting Polymer PEDOT for the Development of Antifouling and Ultrasensitive Electrochemical DNA sensor. *Biosens. Bioelectron.* **2017**, *92*, 396−401.
(34) Niu, Z.; Zhao, Y.; Sun, W.; Shi, S.; Gong, Y. Biomimetic Surface Modification of Polypropylene by Surface Chain Transfer Reaction Based on Mussel-inspired Adhesion Technology and Thiol Chemistry. *Appl. Surf. Sci.* **2016**, *386*, 41−50.
(35) Lu, L. M.; Zhang, X. B.; Kong, R. M.; Yang, B.; Tan, W. A Ligation-triggered DNAzyme Cascade for Amplified Fluorescence Detection of Biological Small Molecules with Zero-background Signal. *J. Am. Chem. Soc.* **2011**, *133*, 11686−11691.
(36) Zhou, S. S.; Zhang, L.; Cai, Q. Y.; Dong, Z. Z.; Geng, X.; Ge, J.; Li, Z. H. A Facile Label-free Aptasensor for Detecting ATP Based on Fluorescence Enhancement of Poly(thymine)-templated Copper Nanoparticles. *Anal. Bioanal. Chem.* **2016**, *408*, 6711−6717.
(37) Liu, Y.; Lei, J.; Huang, Y.; Ju, H. Off-On" Electrochemiluminescence System for Sensitive Detection of ATP via Target-induced Structure Switching. *Anal. Chem.* **2014**, *86*, 8735−8741.
(38) Huang, X.; Li, Y.; Zhang, X.; Zhang, X.; Chen, Y.; Gao, W. An Efficient Signal-on Aptamer-based Biosensor for Adenosine Triphosphate Detection Using Graphene Oxide Both as an Electrochemical and Electrochemiluminescence Signal Indicator. *Analyst* **2015**, *140*, 6015−6024.
(39) Lu, L.; Si, J. C.; Gao, Z. F.; Zhang, Y.; Lei, J. L.; Luo, H. Q.; Li, N. B. Highly Selective and Sensitive Electrochemical Biosensor for

DOI: 10.1021/acsami.7b09529
ACS Appl. Mater. Interfaces 2017, 9, 31153−31160

ATP Based on the Dual Strategy Integrating the Cofactor-dependent Enzymatic Ligation Reaction with Self-Cleaving DNAzyme-amplified Electrochemical Detection. *Biosens. Bioelectron.* **2015**, *63*, 14−20.
(40) Wang, L.; Xu, M.; Han, L.; Zhou, M.; Zhu, C.; Dong, S. Graphene Enhanced Electron Transfer at Aptamer Modified Electrode and Its Application in Biosensing. *Anal. Chem.* **2012**, *84*, 7301−7307.
(41) Tang, J.; Tang, D.; Zhou, J.; Yang, H.; Chen, G. Nuclease Cleavage-assisted Target Recycling for Signal Amplification of Free-label Impedimetric Aptasensors. *Chem. Commun.* **2012**, *48*, 2627−2629.
(42) Yu, P.; He, X.; Zhang, L.; Mao, L. Dual Recognition Unit Strategy Improves the Specificity of the Adenosine Triphosphate (ATP) Aptamer Biosensor for Cerebral ATP Assay. *Anal. Chem.* **2015**, *87*, 1373−1380.
(43) Chen, S.; Cao, Z.; Jiang, S. Ultra-low Fouling Peptide Surfaces Derived from Natural Amino Acids. *Biomaterials* **2009**, *30*, 5892−5896.

DOI: 10.1021/acsami.7b09529
ACS Appl. Mater. Interfaces 2017, 9, 31153−31160